ChemComm

TiO$_2$ nanotubes with ultrathin walls for enhanced water splitting†

Ahmad M. Mohamed,[a] Amina S. Aljaber,[b] Siham Y. AlQaradawi[b] and Nageh K. Allam*[a]

We demonstrate, for the first time, the synthesis of titania nanotubes with ultrathin (3–5 nm) wall thickness. As revealed by the incident photon-to-current collection efficiency (IPCE) and electrochemical impedance spectroscopy measurements, the ultrathin walls, less than the charge carrier diffusion length, were essential to ensure fast and efficient charge carrier collection.

One-dimensional metal oxide nanoarchitectures have demonstrated great performance in many technologies including solar energy conversion.[1–3] In particular, TiO$_2$ nanotube arrays formed by electrochemical anodization have demonstrated outstanding performance in solar fuel generation and solar cell applications.[4,5] Although the use of nanotubular form decouples the light absorption and the transfer of charge carriers, enhancing the dynamics of charge carriers in TiO$_2$ is still a challenge.[6,7] In this regard, many studies have been devoted to improve the dynamics including passivation of defects,[8] the use of co-catalysts among others.[9,10] As many studies have shown the dependence of the functionality of the material on its physical dimensions, the best way to improve the transport and collection of charge carriers is to optimize the inherent intrinsic properties of the material.[7,11,12] To this end, controlling the length and the diameter of TiO$_2$ nanotubes has shown tremendous positive effects on the performance of the materials in solar energy conversion.[12–14] However, the effect of wall thickness was poorly discussed in the literature, despite the fact that it is one of the determinant factors controlling the dynamics of charge carriers, especially in photo-electrochemical water splitting systems.[7,11,14,15] Most of the published articles deal with wall thicknesses that are greater than the diffusion length of charge carriers in titania.[7] Herein, we report the first demonstration of the fabrication of vertically aligned titania nanotube arrays with very thin wall thickness (3–5 nm) and their use in solar water splitting. The thin-walled nanotubes facilitate the diffusion of the photogenerated holes to the semiconductor/electrolyte interface during water splitting, allowing for efficient separation of charge carriers.

The diffusion length of charge carriers in titania is around 10 nm,[7] and until now there has been no reproducible method to produce titania nanotubes with a wall thickness that is considerably lower than the diffusion length. Inspired by the work of Amer *et al.*,[16] who were able to fabricate thin-walled ZrO$_2$ nanotubes, we used a mixture of non-aqueous (glycerol) and aqueous (water) electrolytes to anodize titanium in order to achieve titania nanotubes with ultrathin walls. The detailed experimental setup and conditions are summarized in the ESI†. In order to show the effect of the wall thickness, two sets of samples were fabricated; namely thick-walled nanotubes (NT1) using the conventional anodization method and thin-walled nanotubes (NT2) using our modified fabrication method, see the ESI† for more details.

Fig. 1 shows FESEM images of the fabricated NT1 and NT2. The thin-walled nanotubes (Fig. 1a) are highly ordered, tightly packed with wall thicknesses ranging between 3 and 5 nm, length of ~1 μm, and an inner diameter of 60 ± 5 nm. In contrast, the thick-walled nanotubes (Fig. 1b) are not well-aligned with irregular outer diameters that contain ridges and circumferential serrations, similar to those usually seen upon anodizing Ti in
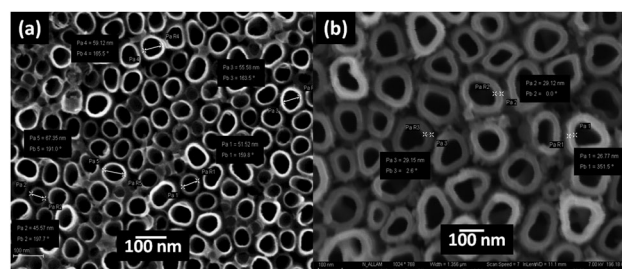
[a] *Energy Materials Laboratory (EML), School of Sciences and Engineering, The American University in Cairo, New Cairo 11835, Egypt. E-mail: Nageh.allam@aucegypt.edu*

[b] *Department of Chemistry and Earth Sciences, Qatar University, Doha, Qatar*

† Electronic supplementary information (ESI) available: Details of the synthesis of thin and thick-walled titania nanotubes. See DOI: 10.1039/c5cc04539h
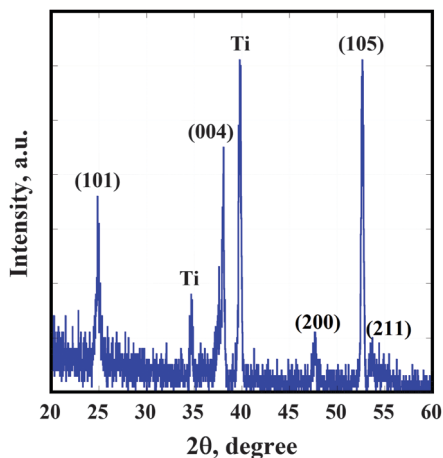

Fig. 1 FESEM images of (a) thin-walled and (b) thick-walled titania nanotubes.

Fig. 2   XRD pattern of the annealed thin-walled nanotubes.

Fig. 3   XPS spectra of thin-walled titania nanotubes.

formamide-based electrolytes. The difference in homogeneity and packing between NT1 and NT2 can be related to the use of highly viscous electrolyte (glycerol) in the case of NT1 as was detailed elsewhere.[14,17,18]

As the as-anodized nanotubes are amorphous, we annealed them in air to crystallize them. Fig. 2 shows the obtained XRD pattern of the annealed thin-walled nanotubes at 450 °C for 4 h. It confirms the crystallization of the titania nanotubes in the regular anatase phase[19] with the appearance of the characteristic diffraction peaks at 25°, 38.1°, 47.8°, 52.8°, and 53.9°, corresponding to the (101), (004), (200), (105), and (211) facets, respectively. Note that unlike thick-walled nanotubes where the predominant facet is (101), the most predominant peak for the thin-walled nanotubes is the (105) crystalline phase. The predominance of the high energy facet (105) increases the hydrogen bonding on the surface of the titania, which results in an increase in the barrier for forming larger crystallites.[20] Scherrer equation is used to calculate the crystallite size. The calculated crystallite size is ∼7.12 nm, with lattice parameters of a = 2.414 nm and c = 3.56 nm, giving a stress along a = 5.38 and along c = 2.74. The relative standard deviation of the determined average particle size is ∼5% and the instrument broadening was corrected for using NIST 640c silicon. Note that the obtained crystallite size for the thin-walled nanotubes (7 nm) is much smaller than that reported for the conventionally prepared thick-walled nanotubes (40–70 nm). Such a small grain size has an effect on the photocatalytic activity of the material as explained later.

To get more insights into the composition of the thin-walled nanotubes, we have performed X-ray photoelectron spectroscopy (XPS) analysis for the annealed samples using a Thermo Scientific K-alpha XPS with an Al anode. Spectra were charge referenced to O 1s at 532 eV. The formation of oxide is evident from the O 1s and Ti 2p peaks with the Ti/O molar ratio being close to the stoichiometric proportion. Note that both Ti 2p$_{3/2}$ and 2p$_{1/2}$ peaks are observed (Fig. 3a) with a separation of 5.7 eV, which confirm the presence of Ti.[4+] The O 1s spectrum (Fig. 3b) is composed of two peaks appearing at 530.9 and 532.1 eV that are characteristic of Ti oxide (Ti–O–Ti) and chemisorbed OH groups on the nanotube's surface, respectively.[20,21]
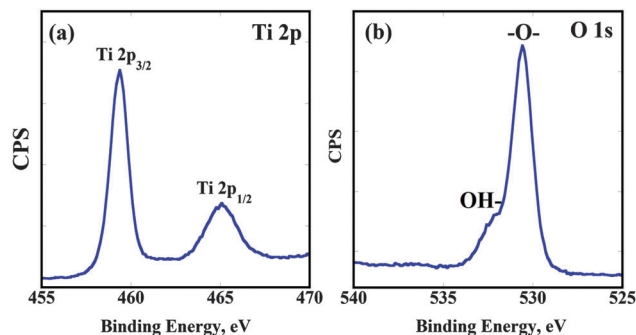
The effect of the wall thickness on the charge carrier dynamics and the performance of titania nanotubes is still unclear in the literature. On one side, it is reported that thick wall thickness would ensure the creation of a large depletion region (space charge region) and consequently there would be enough electric potential difference between the sides of the wall (potential drop).[7,11] The generated electric field in that case would directly result in separation of charge carriers and prevention of recombination.

The potential drop ($\Delta\varphi_o$) across the wall thickness can be calculated using

$$\Delta\Phi_0 = kTr_0{}^2/6eL_D \qquad (1)$$

where r is half the wall thickness and L_D is the Debye length, which can be calculated using

$$L_D = [\varepsilon_0 \varepsilon kT/2e^2 N_D]^{1/2} \qquad (2)$$

where N_D is the charge carrier density, ε and ε_0 are the dielectric constant and the permittivity in air for titania, respectively (23). In this case, there must be a minimal band bending of 50 mV in order to prevent the charge recombination.[11] This band bending (ω) can be consumed by having an efficient depletion region to accommodate the band bending, which can be calculated using

$$\omega = \sqrt{\frac{2\varepsilon\varepsilon_0 V_B}{eN_D}} \qquad (3)$$

where V_B is the amount of band bending. As the wall thickness of the nanotubes supports only a potential depletion zone that is half its width, a wall thickness of ∼24 nm is needed.[7,11]

On the other side, a thinner wall thickness would result in a lower band bending with the band potential being very close to the flat band potential. However, the thin wall thickness would prevent the formation of a large depletion region, and consequently there would not be enough potential drop across the wall, leading to less separation of the photogenerated charge carriers.[7,22] When the wall thickness is less than the diffusion length in titania, which is thought to be about 10 nm, only in this case, there is no electric diffusion layer needed to separate electrons and holes, as the holes simply diffuse through the tube walls to the semiconductor/electrolyte interface,[7] see Scheme 1.

To test the validity of either assumptions mentioned above, the thin-walled and thick-walled titania nanotubes have been
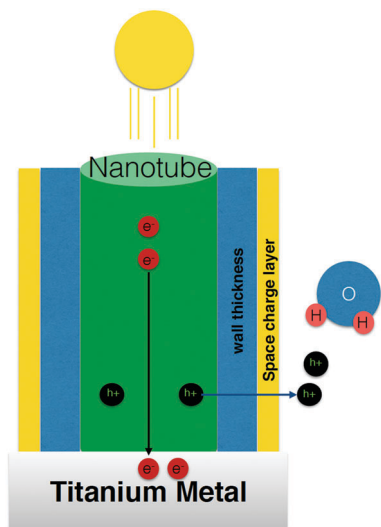
Scheme 1 Pathways of charge carriers in thin-walled titania nanotubes upon illumination. The space charge layer is too small to support the large potential drop across wall thickness, however, the small wall thickness allows efficient hole diffusion at the electrode/electrolyte interface.

used as photoanodes in a three electrode electrochemical cell to split water in a 1.0 M KOH electrolyte solution. Fig. 4a shows the variation of the photocurrent density *versus* applied bias. The photocurrent produced by the thin-walled titania nano-tubes is almost twice that produced by thick-walled nanotubes under the same conditions, highlighting the better charge dynamics for the thin-walled nanotubes. However, the dark current in the case of thick-walled nanotubes is lower than that of the thin-walled counterparts. The high dark current in the case of thin-walled nanotubes can be related to the smaller crystallite size (7 nm) compared to that of thick walls (40–60 nm). Small crystallite size produces a large number of under coordinated Ti atoms on the grain surface. In order to counteract this down coordination, Ti atoms absorb water molecules, leading to the distortion of the crystal structure. This distortion results in the heading of the negative centres to the interior of the grain and the positive centres to the outside, which can be manifested by the formation of parallel surface defect dipole and the increase of dipole–dipole repulsion.[20,21] This defect dipole was shown to increase the dark current.[23] Another privilege of the thin-walled nanotubes is that the onset potential is lower than that for the
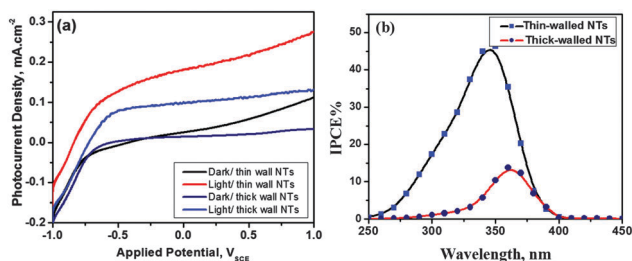
Fig. 4 (a) *I*–*V* and (b) IPCE characteristics of thin-walled and thick-walled titania nanotubes measured in 1 M KOH aqueous solution under dark and illuminated (AM 1.5) conditions.

thick-walled nanotubes. This can mainly be attributed to the better charge kinetics and lower resistance as confirmed later *via* electrochemical impedance measurements.[24]

Incident photon to current collection efficiency (IPCE) experiments were performed without an applied bias in order to better understand the charge carrier collection efficiency in both thin- and thick-walled nanotubes. The experiments were performed in a two-electrode cell with the nanotube film as the working photoelectrode and platinum foil as a counter electrode in 1.0 M KOH solution. The IPCE was calculated using eqn (4), where λ is the wavelength of the incident light, j_{ph} is the photocurrent density under illumination at λ and I_o is the incident light intensity at λ.

$$\text{IPCE}\% = \frac{\left| j_{ph}(\text{mA cm}^{-2}) \right| \times 1239.8(V \times \text{nm})}{I_O(\text{mW cm}^{-2}) \times \lambda(\text{nm})} \times 100 \quad (4)$$

Fig. 4b shows the obtained IPCE, where the thin-walled nanotubes show higher collection efficiency (47%) than the thick-walled nanotubes (15%). These results clearly show the direct effect of reducing the wall thickness on enhancing the charge carrier separation and collection. Also, it is evident that controlling the tube thickness is more effective than relying on the potential depletion region for thick-walled nanotubes.

Another factor that should be considered is the surface area of the nanotubes, which is directly related to their geometrical features. Our calculations showed the superiority of the fabri-cated thin-walled nanotubes over the thick-walled counterparts. The thin walled titania nanotubes have a geometric roughness factor (G) of 185 compared to 60 for the thick-walled nanotubes. More details on the calculations are available in the ESI.†

To get more insights into the effect of wall thickness on the properties of titania nanotubes, electrochemical impedance spectro-scopy (EIS) measurements were done using Biologic SV-200 potentiostat for both thin- and thick-walled nanotubes. The EIS measurements were performed in 1 M KOH electrolyte at room temperature (22 ± 2 °C) under dark conditions. A three-electrode electrochemical cell was used with the nanotube as the working electrode, Pt as the counter electrode and calomel as the reference electrode. The applied voltage was swept from −1 V to 0.6 V, while the frequency ranged from 100 mHz to 1000 KHz.

Fig. 5 shows the obtained Nyquist plots. The thin-walled titania shows higher conductivity compared to the thick-walled counterparts, which confirms the efficient charge carrier transport for the thin-walled nanotubes. This was asserted by the Mott–Schottky analysis, which revealed a flat band potential of −0.7 V *versus* SCE with a charge carrier density of 5×10^{18} cm^{-3}. The obtained flat band potential and carrier density are in agreement with those reported in the literature.[25,26]

In summary, a new synthetic approach to produce thin-walled titania nanotubes, with wall thickness less than the charge carrier diffusion length, is presented. The calculated crystallite size for the thin-walled nanotubes is as small as 7 nm, leading to the creation of a large number of under coordinated Ti atoms on the grain surface and consequently high dark current. The thin-walled nanotubes showed almost double the photocurrent
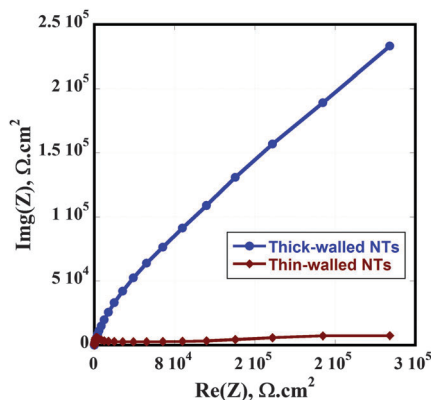
Fig. 5 Nyquist plot of both thin and thick-walled titania nanotubes.

of the thick-walled nanotubes upon their use in water splitting arrangement. The IPCE and electrochemical impedance measurements confirmed the superiority of the thin-walled nanotubes over their thick-walled counterparts. The Mott–Schottky analysis revealed a flat band potential of -0.7 V *versus* SCE with a charge carrier density of 5×10^{18} cm^{-3}. Our work confirmed the importance of using ultra thin-walled titania nanotubes as photoanodes for efficient solar water splitting.

Notes and references

1 B. S. Shaheen, H. G. Salem, M. A. El-Sayed and N. K. Allam, Thermal/Electrochemical Growth and Characterization of One-Dimensional ZnO/TiO$_2$ Hybrid Nanoelectrodes for Solar Fuel Production, *J. Phys. Chem. C*, 2013, **117**, 18502–18509.
2 C. A. Grimes, O. K. Varghese and S. Ranjan, *Light, water, hydrogen: the solar generation of hydrogen by water photoelectrolysis*, Springer, New York, 2008.
3 K. Lee, A. Mazare and P. Schmuki, One-Dimensional Titanium Dioxide Nanomaterials: Nanotubes, *Chem. Rev.*, 2014, **114**, 9385–9454.
4 N. M. Deyab, P. Steegstra, A. Hubin, M. P. Delplancke, H. Rahier and N. K. Allam, Influence of electrolyte composition on the formation of mixed oxide nanotube arrays for solar fuel production, *J. Power Sources*, 2015, **280**, 339–346.
5 W. Sharmoukh and N. K. Allam, TiO$_2$ nanotube-based dye-sensitized solar cell using new photosensitizer with enhanced open-circuit voltage and fill factor, *ACS Appl. Mater. Interfaces*, 2012, **4**, 4413–4418.
6 Anonymous, *Photoelectrochemical Hydrogen Production*, Springer US, Boston, MA, 2012, vol. 102.
7 C. A. Grimes and G. K. Mor, *TiO$_2$ Nanotube Arrays: Synthesis, Properties, and Applications,* Springer-Verlag, Boston, MA, 2009.
8 L. Tsui, M. Saito, T. Homma and G. Zangari, Trap-state passivation of titania nanotubes by electrochemical doping for enhanced photoelectrochemical performance, *J. Mater. Chem. A*, 2015, **3**, 360–367.
9 H. A. Hamedani, N. K. Allam, M. A. El-Sayed, M. A. Khaleel, H. Garmestani and F. M. Alamgir, An Experimental Insight into the Structural and Electronic Characteristics of Strontium-Doped Titanium Dioxide Nanotube Arrays, *Adv. Funct. Mater.*, 2014, **24**, 6783–6796.
10 B. Yang, C. K. Ng, S. Fung, M. K. Fung, C. C. Ling and A. B. Djurišić, Annealing study of titanium oxide nanotube arrays, *Mater. Chem. Phys.*, 2011, **130**, 1227–1231.
11 X. Gao, J. Chen and C. Yuan, Enhancing the performance of free-standing TiO$_2$ nanotube arrays based dye-sensitized solar cells *via* ultraprecise control of the nanotube wall thickness, *J. Power Sources*, 2013, **240**, 503–509.
12 M. Paulose, K. Shankar, S. Yoriya, H. Prakasam, O. Varghese, G. Mor, T. Latempa, A. Fitzgerald and C. Grimes, Anodic growth of highly ordered TiO$_2$ nanotube arrays to 134 μm in length, *J. Phys. Chem. B*, 2006, **110**, 16179–16184.
13 H. Prakasam, K. Shankar, M. Paulose, O. Varghese and C. Grimes, A new benchmark for TiO$_2$ nanotube array growth by anodization, *J. Phys. Chem. C*, 2007, **111**, 7235–7241.
14 S. Liang, J. He, Z. Sun, Q. Liu, Y. Jiang, H. Cheng, B. He, Z. Xie and S. Wei, Improving Photoelectrochemical Water Splitting Activity of TiO2 Nanotube Arrays by Tuning Geometrical Parameters, *J. Phys. Chem. C*, 2012, **116**, 9049–9053.
15 C. Wu, Y. Zhuo, P. Zhu, B. Chi, J. Pu and J. Li, Tunable Fabrication of TiO$_2$ Nanotube Arrays with High Aspect Ratio and its Application in Dye Sensitized Solar Cell, *J. Inorg. Mater.*, 2009, **24**, 897–901.
16 A. W. Amer, S. M. Mohamed, A. M. Hafez, S. Y. AlQaradawi, A. S. Aljaber and N. K. Allam, Self-assembled zirconia nanotube arrays: fabrication mechanism, energy consideration and optical activity, *RSC Adv.*, 2014, **4**, 36336–36343.
17 P. Kar, Effect of anodization voltage on the formation of phase pure anatase nanotubes with doped carbon, *Inorg. Mater.*, 2010, **46**, 377–382.
18 J. Kapusta-Kolodziej, O. Tynkevych, A. Pawlik, M. Jarosz, J. Mech and G. Sulka, Electrochemical growth of porous titanium dioxide in a glycerol-based electrolyte at different temperatures, *Electrochim. Acta*, 2014, **144**, 127–135.
19 G. H. Du, Q. Chen, R. C. Che, Z. Y. Yuan and L. Peng, Preparation and structure analysis of titanium oxide nanotubes, *Appl. Phys. Lett.*, 2001, **75**, 3702–3704.
20 S. Bhattacharya and M. Ahmad, Size effect on the lattice parameters of nanocrystalline anatase, *Appl. Phys. Lett.*, 2009, **95**, 191906.
21 G. Li, J. Boerio-Goates, B. F. Woodfield and L. Li, Evidence of linear lattice expansion and covalency enhancement in rutile TiO$_2$ nanocrystals, *Appl. Phys. Lett.*, 2004, **75**, 2059–2061.
22 J. Macak, H. Tsuchiya and P. Schmuki, High-aspect-ratio TiO$_2$ nanotubes by anodization of titanium, *Angew. Chem., Int. Ed.*, 2005, **44**, 2100–2102.
23 A. Stiff-Roberts, Z. Zhao, C. Yi and K. Lantz, Effect of donor-complex-defect-induced dipole field on In As/Ga As quantum dot infrared photodetector activation energy, *Appl. Phys. Lett.*, 2007, **90**, 233511.
24 Q. Liu, J. He, T. Yao, Z. Sun, W. Cheng, S. He, Y. Xie, Y. Peng, H. Cheng and Y. Sun, Aligned Fe$_2$TiO$_5$-containing nanotube arrays with low onset potential for visible-light water oxidation, *Nat. Commun.*, 2014, **5**, 5122.
25 R. Van de Krol, A. Goossens and J. Schoonman, Mott–Schottky Analysis of Nanometer-Scale Thin-Film Anatase TiO$_2$, *J. Electrochem. Soc.*, 1997, **144**, 1723–1727.
26 Z. Endut, M. Hamdi and W. Basirun, An investigation on formation and electrochemical capacitance of anodized titania nanotubes, *Appl. Surf. Sci.*, 2013, **280**, 962–966.